Journal of Fluorine Chemistry 130 (2009) 102–107

Contents lists available at ScienceDirect

Journal of Fluorine Chemistry

journal homepage: www.elsevier.com/locate/fluor

Selected topics of molten fluorides in the field of nuclear engineering

Takuya Goto *, Toshiyuki Nohira, Rika Hagiwara, Yasuhiko Ito

Department of Fundamental Energy Science, Graduate School of Energy Science, Kyoto University, Sakyo, Kyoto 6068501, Japan

ARTICLE INFO

Article history:
Received 15 March 2008
Received in revised form 10 July 2008
Accepted 15 July 2008
Available online 30 July 2008

Keywords:
Molten fluoride
Electrochemical process
Decontamination
Zirconium

ABSTRACT

A new reference electrode in fluoride melts and a new concept for a spent zircaloy wastes treatment using a mixture of fluoride and chloride melt are proposed. Electrochemical formation of Au_2Na on Au wire in a LiF–KF–NaF shows the equilibrium potential of the reaction: $2Au + Na^+ + e^- = Au_2Na$ at 0.535 V vs. K^+/K in LiF–NaF–KF eutectic melt at 773 K. The (Au_2Na + Au) electrode demonstrates excellent characteristics as a reference electrode in terms of reproducibility, stability and reversibility. LiF–LiCl–KCl melt enhances dissolution and deposition rate of zirconium, which enable us to develop a new decontamination process for a spent zircaloy. Electrochemical decontamination using LiF–LiCl–KCl melt is experimentally achieved a clearance level.

1. Introduction

Molten salts are widely applied to the nuclear engineering field, such as liquid fuel, coolant, electrolyte for producing and reprocessing of nuclear materials and so on. A vast range of support works and studies have thus been done for more than 60 years and most studies are related to molten fluorides because of their excellent physico-chemical properties [1]. The drawback of fluoride melts, however, still remains, roughly classifying into two categories: (1) reference electrodes for some fluoride melts have not been established and thereby data obtained by using uncertain electrode or quasi reference electrode are unacceptable from thermodynamic points of view and (2) solidified fluorides contaminating the object materials are difficult to be removal at room temperature due to low solubility of solid fluorides in aqueous solution. Thus, there are still some rooms for research and development on molten fluoride processing. In the following, the attractive possibilities on fluoride melt from both fundamental and practical aspects will be described to focus two topics recently done by the present authors.

2. Reference electrode for a LiF–KF–NaF melt [2]

2.1. Necessity of a reference electrode for a LiF–KF–NaF eutectic melt

Among many kinds of molten fluorides, a LiF–NaF–KF eutectic melt (LiF:NaF:KF = 46.5:11.5:42.0 mol%, m.p. = 732 K) is the most systematically studied melt in the field of electrochemistry [1]. However, precise and quantitative electrochemical study is rather difficult to conduct in this system due to lack of a good reference electrode. Although several reference electrode systems such as the Ni(II)/Ni in a boron nitride compartment have been tested [3], there is no reference electrode which has thermodynamical significance, excellent stability, durability, reversibility, reproducibility and simple structure. The long-range instability of the electrode was due to reaction of electrode materials with fluoride [3].

In this study, the electrochemical behavior of Au electrode and the electrochemical formation of Au–Na alloy in the melt are first studied. Since the Au–Na alloy shows a very stable potential, it is suggested to be used as a stable reference electrode in a LiF–NaF–KF eutectic melt. Therefore, the main characteristics of (Au_2Na + Au) reference electrode, such as reproducibility, stability and reversibility, are then investigated.

2.2. Cathodic limit of LiF–KF–NaF

According to the literature [4–8], the cathodic limit at Pt, Ni and Cu electrodes in the LiF–NaF–KF eutectic melt has been suggested to be the deposition of potassium. However, no experimental evidence has been shown so far. Therefore, the potentials of Li^+/Li, Na^+/Na and K^+/K are measured using each alkali metal electrode in the LiF–NaF–KF eutectic melt. In order to determine the cathodic limit of the melt at the nickel electrode, Li, Na, K metal electrodes were designed for measuring the potential of Li^+/Li, Na^+/Na and K^+/K, respectively. A nickel wire spot-welded to porous Ni at the bottom was inserted in an alumina tube. Alkaline metals (Li, K, Na)

* Corresponding author.
E-mail address: goto@energy.kyoto-u.ac.jp (T. Goto).

0022-1139/$ – see front matter © 2008 Elsevier B.V. All rights reserved.
doi:10.1016/j.jfluchem.2008.07.016

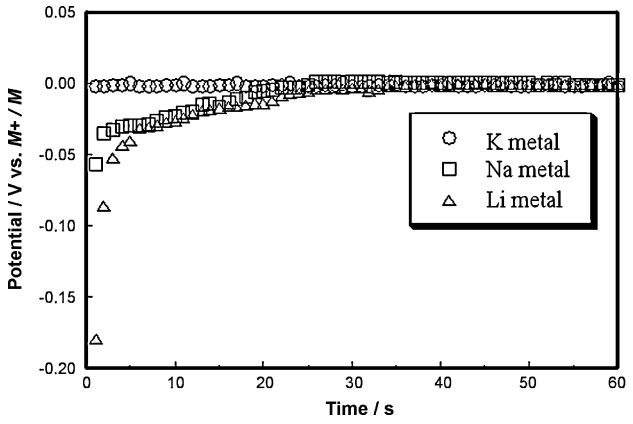

Fig. 1. Potential transient curves of Li, Na and K metal electrode in a LiF–NaF–KF eutectic melt at 773 K [2].

were directly into the tube and then the potentials were recorded, respectively. Fig. 1 shows the obtained potential transient curves for the alkali metal electrodes against the potential of the M^+/M (M = alkali metal electrodeposited on a Ni electrode) dynamic reference electrode. The potential of K^+/K coincides well with that of M^+/M. The potentials of Li^+/Li and Na^+/Na are more negative than the potential of M^+/M in the beginning. After 30 s, the potentials of Li^+/Li and Na^+/Na recover to the same potential as that of M^+/M. The observed potential shifts are explained by the displacement reaction occurring on the Li and Na electrodes. These results demonstrate the cathodic limit at Ni electrode in the LiF–NaF–KF eutectic melt corresponding to the deposition of potassium. Therefore, electrode potentials are hereafter expressed with reference to the K^+/K dynamic reference electrode prepared by electrodepositing potassium metal on a Ni electrode.

2.3. Electrode behavior of Au

The electrode behavior of Au is investigated by cyclic voltammetry at 773 K. The obtained voltammogram is shown in Fig. 2. Large cathodic current at 0 V and large anodic current at 3.8 V correspond to the deposition of alkali metals and the dissolution of Au, respectively. Besides these currents, a pair of redox peaks was observed at around 0.5 V. The peaks are considered to correspond to the formation of Au-alkali metal alloy and anodic dissolution of alkali metal from the alloy, respectively. Open-circuit potentiometry is conducted to further investigate the alloy formation. Open-circuit potential transient curve are recorded at a Au electrode after electrolysis at 0 V for 300 s in a LiF–KF–NaF eutectic melt at 773 K. Since the deposited alkali metal diffuses into the inside of the Au electrode, the electrode potential gradually shifts to more positive values. The observed stable potential plateau at 0.535 V is considered to be attributed to the existence of coexisting phase of Au-alkali metal alloy.

Based on these results, potentiostatic cathodic electrolysis is conducted at a Au electrode at 0.3 V for 2 h to obtain the alloy sample. The XRD pattern of this sample is ascribed to Au_2Na (cubic unit cell, a = 0.779 nm), indicating that the cathodic current peak at 0.45 V in Fig. 2 corresponds to the formation of Au_2Na phase. According to the phase diagram of Au–Na system [9], only Au_2Na alloy exists as a solid alloy at the experiment temperature below 1275 K. In order to examine the anodic reaction at 0.6 V, potentiostatic anodic electrolysis is conducted at 0.6 V for 1 h using the previously formed Au_2Na electrode. The obtained sample is also analyzed by XRD, which shows the existence of only Au. From these results, the pair of redox peaks in Fig. 2 and the potential plateau at 0.535 V of the open-circuit voltammogram are proved to correspond to the following reaction:

$$2Au + Na^+ + e^- = Au_2Na \quad (1)$$

Deposited potassium metal at cathodic limit is chemically substituted with Au_2Na during the experiment, because Au_2Na is thermodynamically stable than potassium metal on a gold electrode. Therefore, reoxidation peak corresponding to the cathodic peak at 0 V is not visible in Fig. 2.

2.4. Durability of (Au_2Na + Au) electrode

Since the (Au_2Na + Au) electrode shows a very stable potential, it is suggested to be used as a stable reference electrode in a LiF–NaF–KF system. Potentiostatic electrolysis is conducted at a Au electrode at 0 V (vs. K^+/K). It suggests that two phases (Au_2Na + Au) coexist. Then, using the (Au_2Na + Au) electrode as a reference electrode, the electrolysis is repeated with another Au electrode under the same conditions. Fig. 3 shows the measured potential transient curve after the electrolysis. The potential difference is observed for about 3 h till coexisting (Au_2Na + Au) phase starts to appear on new Au electrode. After that, the potential difference remains within 1 mV and lasted more than 25 h. This result shows that (Au_2Na + Au) reference electrode has good stability and reproducibility. A reliability reference electrode must give a fixed

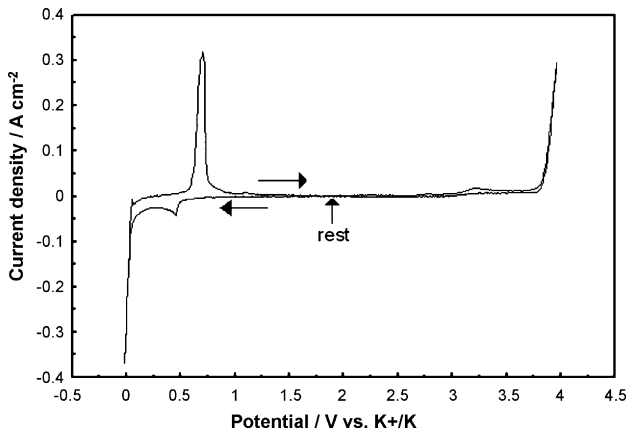

Fig. 2. Cyclic voltammogram at Au electrode in a LiF–NaF–KF eutectic melt at 773 K. Scan rate: 0.1 V s^{-1} [2].

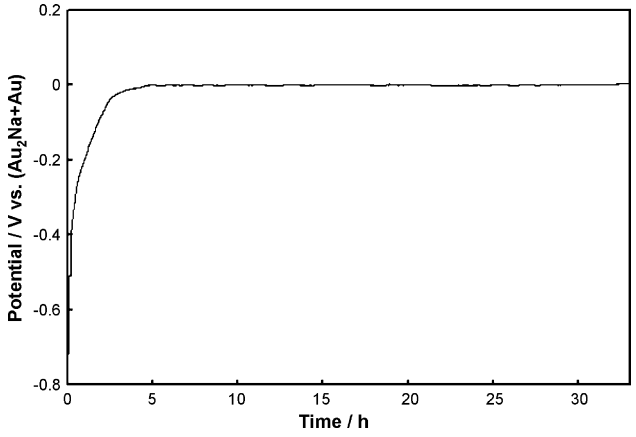

Fig. 3. Open-circuit potential transient curve of a Au electrode after electrolysis at 0 V for 600 s in a LiF–NaF–KF eutectic melt at 773 K [2].

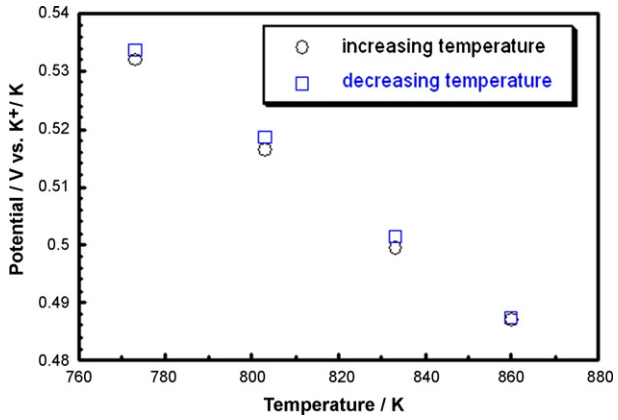

Fig. 4. Relationship between the equilibrium potential of (Au_2Na + Au) electrode and temperature [2].

equilibrium potential value at a specified temperature, that is, the potential of the (Au_2Na + Au) electrode is maintained identical under the conditions of both increasing and decreasing the temperature. No temperature hysteresis is observed as shown in Fig. 4.

3. Electrochemical decontamination of spent zircaloy cladding and channel boxes from boiling water reactors

3.1. Electrochemical decontamination from spent zircaloy

Zircaloy is a kind of zirconium based metal mainly consisting of about 98% Zr, which is widely used as cladding and channel boxes in nuclear plants. Spent zircaloy using at boiling water reactors (BWR) is treated as nuclear waste material, although spent nuclear fuel is recycled and recovered. The disposal costs of zircaloy wastes were estimated to be more than 400 billion yen because they require the deep disposal as the high-βγ wastes generated from the spent fuel reprocessing plant at Rokkasho in Aomori, Japan. If decontamination of spent zircaloy were possible, nuclear grade zirconium would be recovered from the decontaminated zircaloy. This might be one of the most effective solutions of the problem for environment issues in field of the nuclear energy engineering.

The electrorefining of zircaloy to recover zirconium is thus proposed. It is expected to have high decontamination factor (DF) and reduces the secondary wastes. Since the redox potentials of Co-60, Sb-125, Nb-95, Mo-93 containing in the spent zircaloy as radioactive nuclides are more positive than that of Zr [10] and thereby only zirconium is dissolved to give zirconium ions in the molten salt and the radioactive nuclides are precipitated at the bottom of an anode basket as hot debris by applying an anodic voltage. After elimination of radioactive nuclides, zirconium ions in the molten salt are recovered at a cathode by applying a cathodic voltage. The purpose of this study is to confirm the feasibility of zirconium recovery from the spent channel boxes after eliminating radioactive nuclides.

Molten chloride is not suitable for this process, because Sakamura reported that zirconium is not dissolved promptly in molten chloride media due to the formation of sub-halide [11]. It was reported by Groult et al. that deposition and dissolution of zirconium in molten fluoride were one-step four electrons reaction [12]. However, molten fluoride is also not appropriate for the electrolyte of the process, because rather complicated chemical treatment is necessary for removing the solidified fluorides on the depositions and should lead to increase the nuclear disposal. Therefore, a mixture of fluoride and chloride having both excellent properties is selected as an electrolyte for this process.

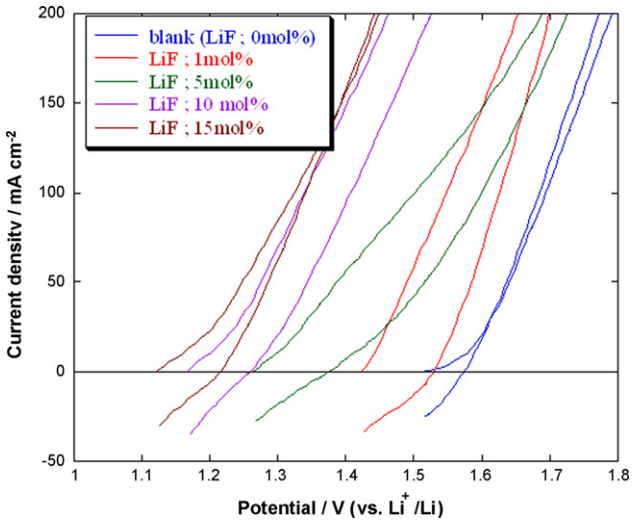

Fig. 5. Cyclic voltammograms for Zr in LiCl–KCl–LiF (0–15 mol%) at 873 K.

In this study, the electrode behavior of zirconium metal has been tested, by changing the additive amount of LiF in a LiCl–KCl eutectic. After selecting a molten salt, electrochemical decontamination was conducted using the irradiated zircaloy samples of channel boxes containing Co-60, Sb-125, Nb-95 and Mo-93 as radioactive nuclides to evaluate DFs.

3.2. Dissolution of zirconium

Cyclic voltammetry of zirconium was conducted to investigate the additive effect of LiF on electrode reaction of zirconium as shown in Fig. 5. The anodic current in the absent of LiF is observed from 1.51 V vs. Li^+/Li, which agrees with the standard redox potential of a Zr(IV)/Zr couple [13]. This indicates that zirconium metal dominantly dissolved as Zr(IV) in a LiCl–KCl melt. The dissolution potential of zirconium decreases with increasing the additive amount of LiF. It seems reasonable that the redox potential of Zr(IV)/Zr shifts toward negative potential direction, because it is reported that a redox potential of Zr(IV)/Zr at about 0.9 V vs. Li^+/Li in LiF–KF–NaF is 0.6 V smaller than that in LiCl–KCl [13].

Galvanostatic electrolysis of zirconium at 50 mA cm^{-2} is conducted in LiCl–KCl containing various LiF concentrations and potential transient curves of a zirconium electrode start to be recorded 100 s after starting electrolysis (Fig. 6). The average potentials decrease with increasing the additive amount of LiF. In the case that LiF is absent in the melt, the observed potential more easily fluctuate. This indicates that zirconium surface is partially covered with passivation layers (probably formation of K_2ZrCl_6 and/or ZrCl) thereby the electrochemical active area is changed momentarily. On the other hand, in the cases that the melts contain LiF, the recorded potentials are smooth, which imply that the electrochemically produced Zr(IV) ions exist mostly as ZrF_6^{2-} in the melts.

3.3. Deposition of zirconium

The reduction of Zr(IV) occurs below about 1.3 V in all cases, judging from the potentials where cathodic currents are observed in Fig. 6. In order to investigate the effect of LiF on the reduction process, two samples are prepared by conducting potentiostatic electrolysis of molybdenum electrodes at 1.2 V for 1 h in LiCl–KCl–LiF (10 mol%)–$ZrCl_4$ (1 mol%) and LiCl–KCl–$ZrCl_4$ (1 mol%), respectively. After terminated electrolysis, obtained samples are rinsed with distilled water to remove the solidified salt on the deposition. The depositions of both samples coincide with metallic zirconium

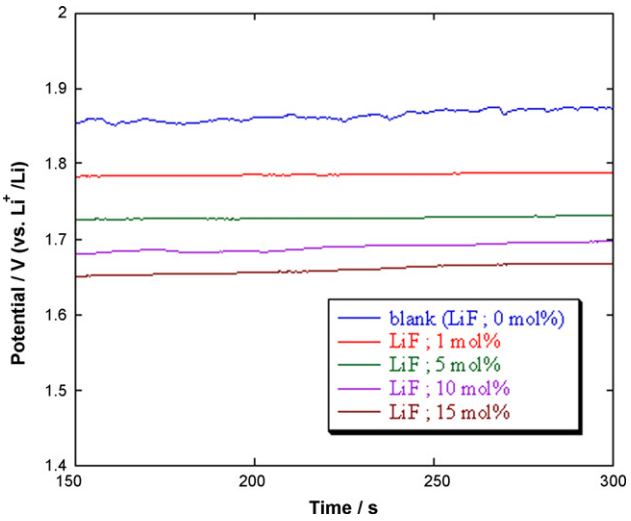

Fig. 6. Potential transient curves of a Zr during galvanostatic electrolysis at 50 mA cm^{-2} in a in LiCl–KCl–LiF (0–15 mol%) at 873 K.

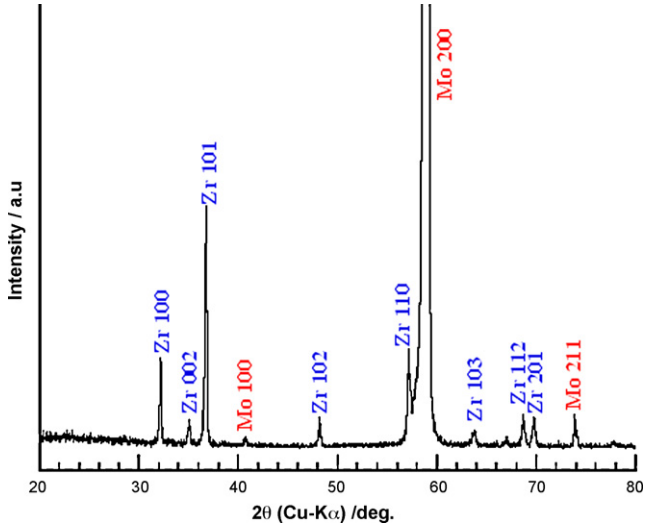

Fig. 7. XRD pattern of a Mo electrode after potentiostatic electrolysis at 1.2 V for 1 h in LiCl–KCl–LiF (10 mol%)–$ZrCl_4$ (1 mol%) at 873 K.

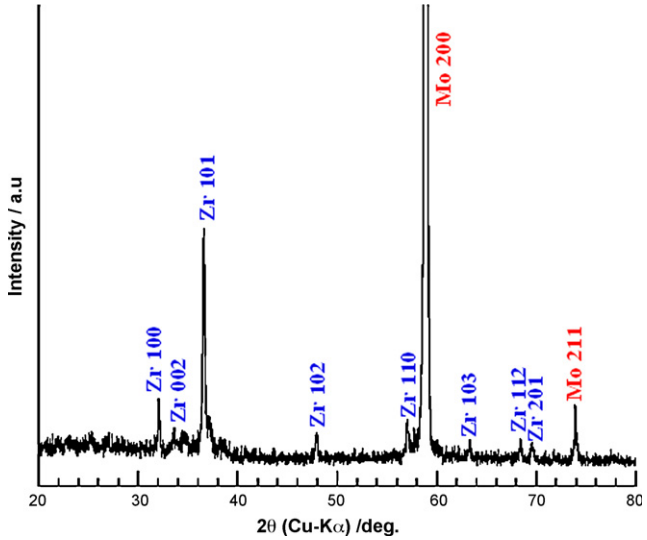

Fig. 8. XRD pattern of a Mo electrode after potentiostatic electrolysis at 1.2 V for 1 h in LiCl–KCl–$ZrCl_4$ (1 mol%) at 873 K.

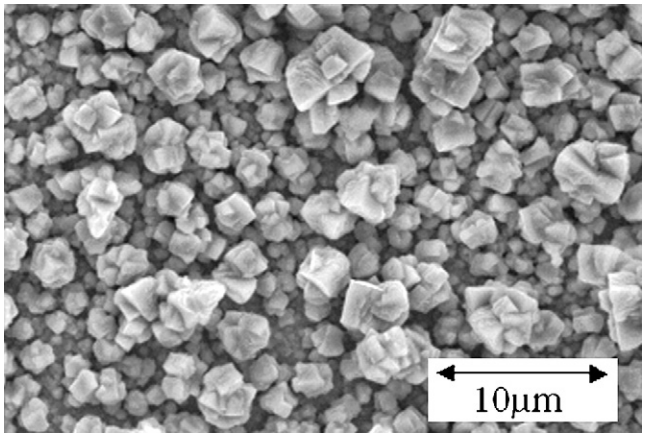

Fig. 9. SEM image of Mo electrode after potentiostatic electrolysis at 1.2 V for 1 h in LiCl–KCl–LiF (10 mol%)–$ZrCl_4$ (1 mol%) at 873 K.

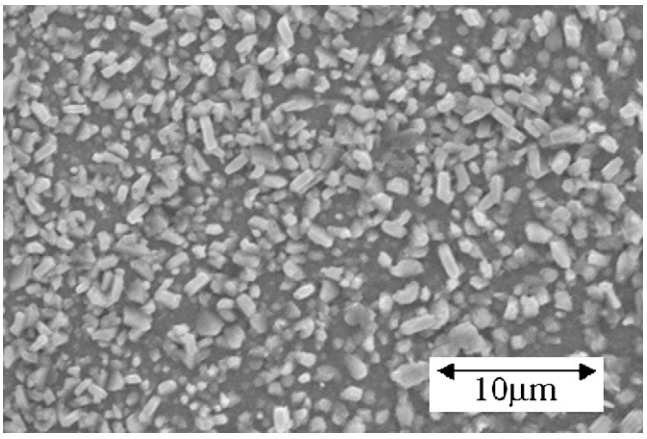

Fig. 10. SEM image of Mo electrode after potentiostatic electrolysis at 1.2 V for 1 h in LiCl–KCl–$ZrCl_4$ (1 mol%) at 873 K.

as shown in Figs. 7 and 8. On the other hand, from surface images of SEM (Figs. 9 and 10), the deposition of zirconium is dense compared to the sample preparing in LiCl–KCl. The difference of surface morphology may occur by changing anion surrounding zirconium cation, corresponding that the surrounding anions change from Cl^- to F^- by adding LiF to the melt. These fundamental studies reveal that dissolution and deposition of zirconium are

Table 1
The radioactivity of the species of actual spent channel box before the electrorefining test [14]

	Radioactivity (Bq g^{-1})
Co-60	3.84×10^6
Sb-125	8.39×10^6
Mb-95	ND
Mo-93	ND

Table 2
Electrorefining test conditions for the first step [14]

Molten salts	LiCl–KCl–LiF
Amount of molten salts (g)	461
Zirconium concentration in salts (w/o)	4.0
Weight of the actual sample (g)	2.51
Anode materials	Stainless steel
Cathode materials	Low carbon steel
Temperature (K)	923
Anode current density (A cm^{-2})	0.1

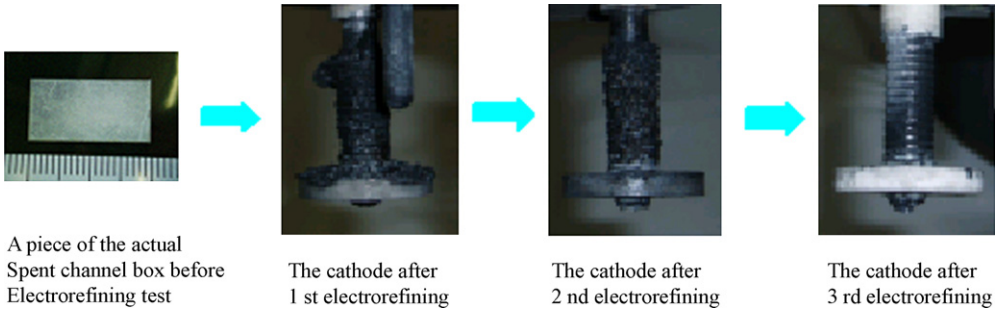

Fig. 11. Photographs of a piece of the spent channel box before electrorefining and the cathodes after electrorefining [14].

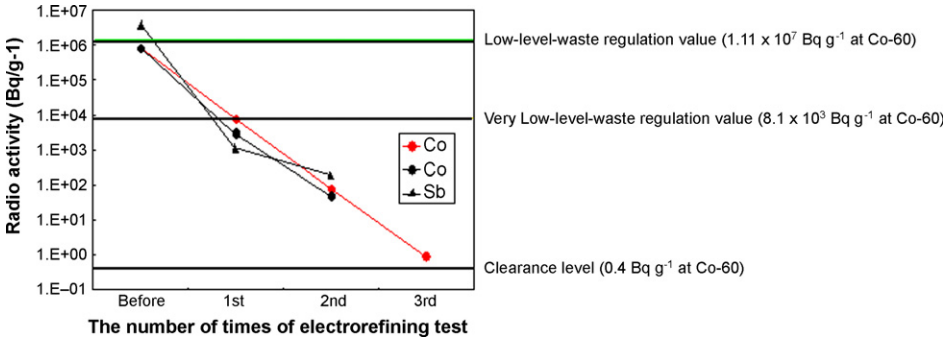

Fig. 12. The results of electrorefining tests in molten salts [14].

enhanced in a mixture of fluoride and chloride melt. A LiCl–KCl eutectic containing 10 mol% LiF at 823 K is thus selected.

3.4. Electrorefining tests using actual samples [14]

The electrorefining tests in LiCl–KCl–LiF(10 mol%) are carried out using actual samples of the spent channel box. Table 1 shows that the radioactivities of the sample before decontamination are measured by γ-spectroscopy. Decontamination factor are defined as a ratio of specific amount of radioactivity before decontamination (Bq g^{-1}) divided by that after decontamination (Bq g^{-1}). The radioactivities of Nb-95 and Mo-93 are not detected due to below the detected level because those activities of Nb-95 and Mo-93 have already decayed. The electrorefining test condition for the first step is shown in Table 2. The zirconium deposited cathode at the first step is used as the anode at the second step. The voltage is applied between the anode and a new cathode at the second step.

Zirconium metal is deposited on the cathode as shown in Fig. 11. Fig. 12 shows that radioactivities of Co-60 and Sb-125 decrease with increasing the number of steps of electrorefining tests. The decontaminated level at the first step of Co-60 is 8.1×10^3 Bq g^{-1} corresponding to the very low-level-waste regulation value. The DF of Co for Zr is calculated to be 4×10^2 for the first step. The decontamination level of Co-60 at the second step is below 1×10^2 Bq g^{-1}. The DF of Co for Zr is thus estimated to be 4×10^4 for the second step of electrorefining. The DF of Co for Zr for the forth step is estimated to be more than 1×10^6, which is derived from a fitting line shown in Fig. 12 on the results of the second step of electrorefining.

4. Conclusions

The results obtained throughout the present study are summarized as follows:

(1) Electrochemical preparing Au_2Na and Au in LiF–KF–NaF melt at 773 K shows that the equilibrium potential of the reaction: $2Au + Na^+ + e^- = Au_2Na$
The above electrochemical couple showed excellent stability and reproducibility by keeping stable potential within 1 mV for 25 h.

(2) A cathode limit at a nickel electrode in LiF–KF–NaF is found to be the deposition of potassium metal. Therefore, the potential of the (Au_2Na + Au) electrode is calibrated vs. K^+/K dynamic reference electrode prepared by electrodepositing potassium metal on a nickel wire.

(3) A new spent zircaloy wastes treatment in a mixture of a fluoride and chloride is proposed and experimentally confirmed their possibilities.

(4) Using a LiF–LiCl–KCl melt enhanced dissolution and deposition of zirconium. Decontamination of zircaloy in a mixture of fluoride and chloride melt is experimentally achieved a very low-level-waste regulation value by means of a proposed electrochemical method.

There are many studies concerning fluoride melts [15,16], however, there are still some rooms for research and development on molten fluoride processing. The studies described in the paper are still at early stages and now are being further continued. Through intensive and systematic studies, processes using molten fluoride in the field of nuclear engineering will become a key technology in the future.

Acknowledgement

The studies were partially supported by a Grant-in-Aid from the Japanese Ministry of Education, Culture, Sports, Science and Technology.

References

[1] D.G. Lovering (Ed.), Molten Salt Technology, Plenum Press, New York, 1982.
[2] H. Quiao, T. Nohira, Y. Ito, Electrochim. Acta 47 (2002) 4543–4549.
[3] H.W. Jenkins, G. Mamantov, J. Electroanal. Chem. 19 (1968) 385–389.
[4] K. Furukawa, A. Lecocq, Y. Kato, K. Mitachi, Nucl. Sci. Technol. 27 (1990) 1157.
[5] D.G. Lovering, R.J. Gale, Molten Salt Techniques, vol. 3, Plenum Press, New York, 1987, pp. 202–213.

[6] D.G. Lovering, R.J. Gale, Molten Salt Techniques, vol. 3, Plenum Press, New York, 1987, pp. 86–87.
[7] F.R. Clayton, G. Mamantov, D.L. Manning, J. Electrochem. Soc. 120 (1973) 1193–1199.
[8] H. Wendt, K. Reuhl, V. Schwarz, Electrochim. Acta 37 (1992) 237–244.
[9] T.B. Massalski, 2nd ed., Binary Alloy Phase Diagrams, vol. 1, ASM International, USA, 1990, pp. 397–398.
[10] R. Fujita, H. Nakamura, N. Kondo, K. Utsunomiya, S. Wada, in: Proceedings of the Seventh International Conference on Nuclear Engineering, Tokyo, (1999), p. 186.
[11] Y. Sakamura, J. Electrochem. Soc. 151 (2004) C187–C193.
[12] H. Groult, A. Barhoun, E.El. Ghallali, S. Borensztjan, F. Lantelme, J. Electrochem. Soc. 155 (2008) E19–E25.
[13] A.J. Bard (Ed.), Encyclopedia of Electrochemistry of the Elements, Marcell Dekker, New York, 1976.
[14] R. Fujita, H. Nakamura, Y. Haraguchi, R. Takahashi, K. Utsunomiya, M. Sato, Y. Ito, T. Goto, T. Terai, S. Ogawa, Transact. Atom. Energy Soc. Jpn. 6 (2007) 343–357 (in Japanese).
[15] J. Uhlir, J. Nucl. Mater. 360 (2007) 6–11.
[16] P. Chamelot, L. Massot, C. Hamel, C. Nourry, P. Taxil, J. Nucl. Mater. 360 (2007) 64–74.